2000-01-2715

Material Modeling Effects on Impact Deformation of Ultralight Steel Auto Body

Srdan Simunovic
Oak Ridge National Laboratory

Jody Shaw
U.S. Steel Corporation

Gustavo A. Aramayo
Oak Ridge National Laboratory

The submitted manuscript has been authored by a contractor of the U.S. Government under contract No. DE-AC05-00OR22725. Accordingly, the U.S. Government retains a nonexclusive, royalty-free license to publish or reproduce the published form of this contribution, or allow others to do so, for U.S. Government purposes.

ABSTRACT

This paper describes the results of the computational analysis of UltraLight Steel Auto Body (ULSAB) crash simulations that were performed using advanced material modeling techniques. The effects of strain-rate sensitivity on a high strength steel intensive vehicle was analyzed. Frontal and frontal offset crash scenarios were used in a finite element parametric study of the ULSAB body structure. Comparisons are made between the crash results using the piece-wise-linear isotropic plasticity strain-rate dependent material model, and the isotropic plasticity material model based on quasi-static properties. The simulation results show the importance of advanced material modeling techniques for vehicle crash simulations due to strain-rate sensitivity and rapid hardening characteristics of advanced high strength steels. Material substitution was investigated for the main frontal crush structure using the material of similar yield stress a significantly different strain-rate and hardening characteristics.

INTRODUCTION

The remarkable evolution of steel technology in recent years has resulted in the development of new High Strength Steel (HSS) materials and processes that are increasingly used in today's automobiles. The combination of formability, strength, ductility, strain-rate sensitivity and strain hardening characteristics of HSS materials indicates their potential to absorb significantly higher amounts of energy during crashes than conventional low-carbon steels, while reducing the overall weight of a vehicle.

The ULSAB [1] is an aggressive attempt of reduction in automobile weight using the existing technologies and materials. ULSAB uses high strength steel and ultra high strength steel for more than 90 percent of the body structure in order to improve structural performance and reduce mass. ULSAB also utilizes new technologies such as hydroforming, tailor-welded steel blanks, steel sandwich materials and laser welding and applies them at performance-critical regions. In order to reduce weight, the ultra-light steel vehicles use fewer and more slender parts placed at the critical positions in the structure. Connections between those parts are also optimized for weight and often involve innovative joining techniques in order to transmit higher level of forces through smaller sections. The reduced number of parts and joints also means that there is less redundancy in the structure. Components that dissipate crash energy have to perform exactly to the specifications of the design team. Therefore, the modeling of these parts has to involve high accuracy and employ realistic material models that will allow vehicle designers to fully explore the potential of increased yield, strain hardening, strain-rate sensitivity, formability, post-form processing and strength of HSS.

The paper outline is as follows: in the next section, brief background information on material modeling for crashworthiness of high strength steels is presented. The following section describes the ULSAB crash model and material models used in the original design. In the next section, material information that was developed by the Auto/Steel Partnership experimental program is described in the context of its applicability to the ULSAB materials. The new material models that incorporate strain-rate sensitivity were incorporated into the ULSAB crash model and the results are discussed in the Crashworthiness Results section. Next, substitution of High Strength Low Alloy (HSLA) 340 steel, which comprises the main frontal crash structure, with Dual Phase (DP) 430 steel is considered, and results from the corresponding crashworthiness simulations are compared to A/SP materials-based design. Strain-rate sensitivity of DP design is assessed by comparing simulations based on quasi-static and strain-rate sensitive material models, respectively. The conclusions of the presented research are stated in the final section.

BACKGROUND

Automotive design, impact mechanics, material and structural science and modeling, and various modeling approaches all come together in the process of development of detailed Finite Element Method (FEM) models of automotive crashes. These fields have advanced so dramatically, driven in large part by the automotive industry, that a general overview of the subject can be achieved by referencing standard textbooks. In-depth discussion of the automotive crashworthiness design and modeling approaches can be found in a review of the state-of-the-art of automobile structural crashworthiness [2]. Analytical treatment and overview of the low velocity impact mechanics can be found in Reference 3. Reference 4 can be used for steel material information, while References 5 and 6 provide comprehensive treatments of material and impact modeling using FEM.

During an axial-type collapse (a.k.a. crush), well-behaved frontal energy dissipation structures collapse approximately to one-fourth of their original length. Dissipation of energy can be related to the magnitude, duration and the time history of the forces sustained in the structure. In current vehicle designs, the brunt of the impact is dissipated by a limited number of components, such as lower and upper car rails. Control of the spatial distribution of impact forces is also important, since it is desirable to align the crush forces with the vehicle center of gravity so that the overturning moment does not compound on the vehicle and the passenger kinematics. Any reduction of the structural redundancy in the energy absorbing structure results in a commensurate requirement for better control of the collapse process in the remaining components. Down gauging using HSS can be viewed as a reduction in structural redundancy as well. It is not difficult to see that understanding of the material response is a primary building block for understanding impact response of a HSS structure.

Strain hardening of the HSS is generally different than that of conventional mild steel materials. In particular, DP and Transformation Induced Plasticity (TRIP) steels exhibit very steep and sustained hardening rates. Rapid strain hardening has the benefits of increased forming limits, increased buckling resistance and increased capacity for impact energy dissipation. However, the increase in the apparent material yield and flow stresses has to be carefully managed because of the resulting increase in peak magnitudes and oscillations of reacting forces in HSS components during an axial collapse. Rapid strain hardening has the effect of wider re-distribution of plastic zones, effectively engaging larger material volumes in the energy dissipation. The size of the plastic regions and formation of the folding patterns may be different than the case of mild steel because of different characteristic lengths of plastic zones that are influenced by material properties. Effect of strain-rate sensitivity (see for example Reference 7) is in some ways similar to strain hardening effect since, for dynamic loading, it raises the magnitude of yield and flow stresses and; consequently, changes redistribution of forces compared to quasi-static loading situation. Rapid strain hardening can result in more diffused plastic zones which influence the strain-rate effects and vice-versa.

There is considerable uncertainty and lack of reliable data for deformation of the HSS under uniaxial dynamic loads. Furthermore, constitutive models for HSS under complex loading conditions have not been established and the data for dynamic multiaxial loading are even scarcer than for the uniaxial case. Therefore, isotropic plasticity constitutive models that have been proven to work well for conventional automotive mild steels and corresponding materials characterization programs have been used in practice. Current vehicle crash models have been developed for conventional mild steel designs and include various dynamic sensitivity parameters that reflect the understanding of the characteristics of mild steel performance and the limitations of the numerical modeling techniques [8-11]. Such modeling experience with HSS is not yet available, although reports have been made on application of engineering approaches for advanced HSS, such as Reference 12. Efforts to characterize the new advanced HSS materials are underway and some of the results are already available from automotive and material producer associations [13]. The materials data developed from these projects were used in development of advanced material models for ULSAB to assess the influence of the modeling approaches on crash response. It must be noted that even with the incredible advances in computer power and modeling theory, every crash simulation model requires experimental validation to fine tune its performance. Nevertheless, the objective of this research was to determine the effect that advanced material models can have on the simulation response and to provide measures that can be used for determining whether the increased experimental and modeling complexity is significant enough to warrant their use in practical design.

ULSAB MATERIALS

The ULSAB vehicle LS-DYNA3D [14] crash model was developed by the Porsche Engineering Services, Inc. (PES) for the ULSAB Consortium [1]. It provided a starting point for the material modeling evaluations. The original ULSAB materials were selected primarily on the basis of their yield values and commercial availability of the formable grades at the time of the design. Most of the crash energy management structures were made of HSLA steels. In fact, 45 percent of the total ULSAB weight is made of a HSLA steel with yield strength of 350 MPa, which is used in all major crash related areas. Specific issues and discussion on selection of steel materials based on required performance characteristics of the ULSAB sub-structures can be found in intermediate reports on the ULSAB project. However, exact designations of steels used were not available, and materials were identified by their yield value only. The original design uses seven different steel materials for sheet metal parts. Material sub-systems for each of the different ULSAB materials are shown in Figures 1 to 7. The materials are denoted with numbers 1-7 and will be referred to in that manner in the remainder of the paper.

Figure 1. ULSAB Material 1.

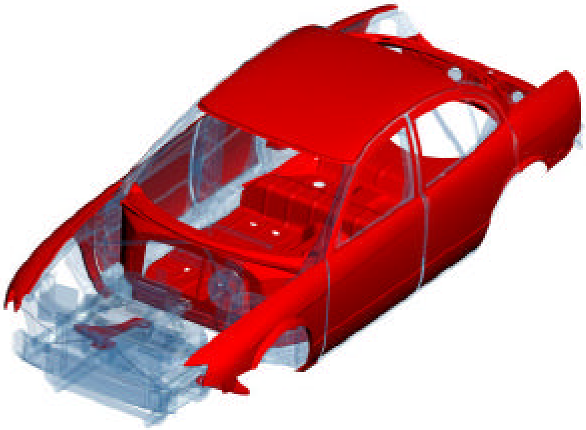

Figure 2. ULSAB Material 2.

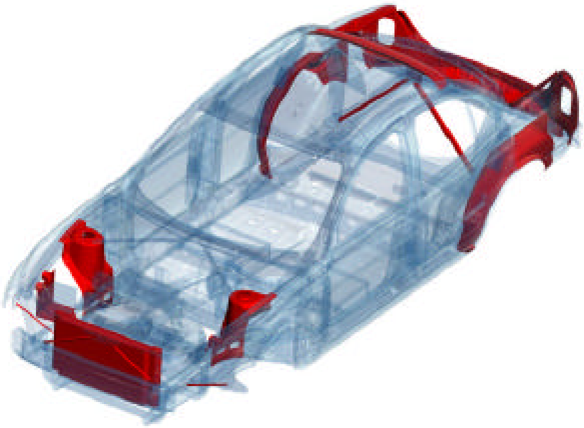

Figure 3. ULSAB Material 3.

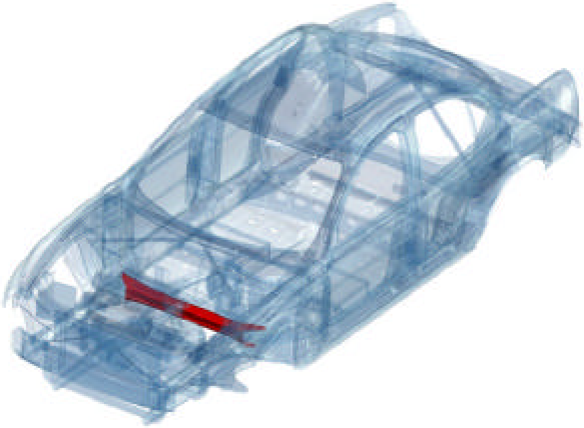

Figure 4. ULSAB Material 4.

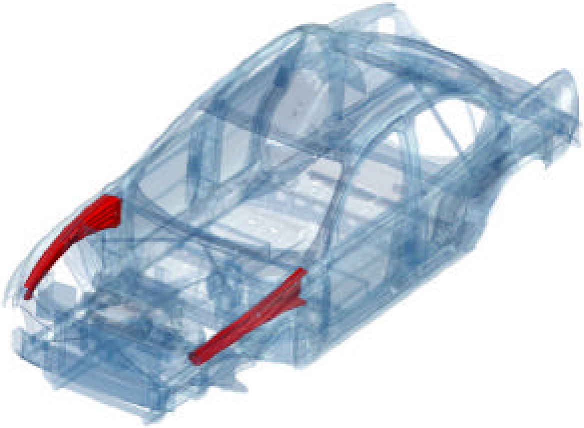

Figure 5. ULSAB Material 5.

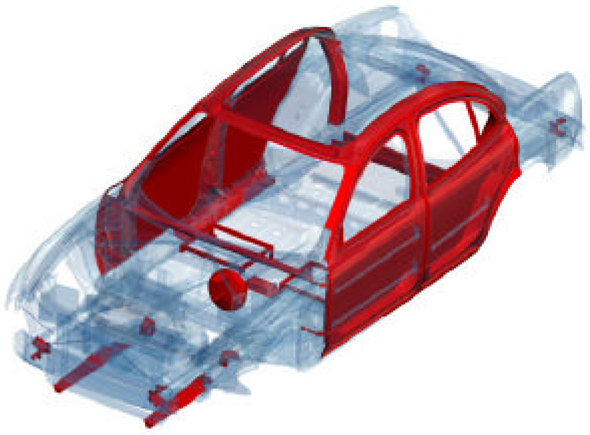

Figure 6. ULSAB Material 6.

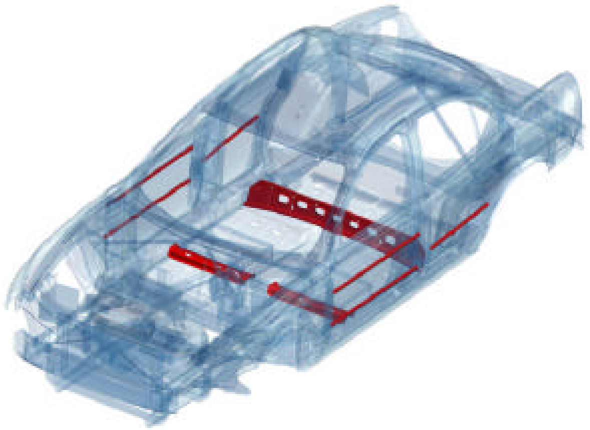

Figure 7. ULSAB Material 7.

The material properties from the original PES model are shown in Figure 8. The material data are based on quasi-static experiments and the corresponding true plastic strain-true plastic stress curves were used as parameters for the piece-wise-linear isotropic plasticity material model (LS-DYNA3D material 24).

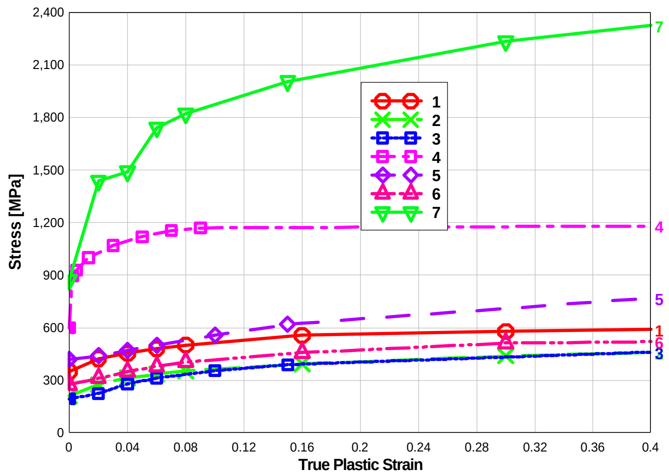

Figure 8. Original ULSAB Material Properties.

ULSAB has been designed to satisfy various safety requirements based on both U.S. and European standards. The scope of the presented research was the analysis of frontal impact situations and, therefore, the focus will be on the frontal energy management structures. Materials 1 and 5 comprise the main frontal safety structure that is designed to absorb frontal impact energy in a controlled manner. The authors used frontal impact into flat rigid barrier with vehicle speed of 35 mph as specified in the U.S. Department of Transportation, New Vehicle Assessment Program (NCAP) test, and frontal impact into flat 50% offset rigid barrier in order to more aggressively engage specific safety structures.

Over the last decade, automotive and steel companies have been developing material properties for the automotive high strength steels under dynamic loading conditions. Spot- and laser-welded steel columns were investigated in Reference 15. Yoshitake et al. [16] used double-hat specimens made out of steels having 440 to 780 MPa tensile strengths and used effective width theory to estimate average forces in the specimens. Sato et al. [17] performed axial compression experiments and corresponding FEM numerical simulations with steel grades of 300 to 590 MPa. The authors used two approaches for material modeling, Cowper-Symonds [7] and piece-wise-linear isotropic plasticity model. Results show better correlation of simulations with experimental for the piece-wise-linear isotropic plasticity model. Miura et al. [18] have shown a good agreement between experiments and FEM simulations for crushing of hat shaped DP specimens. However, particulars of the material models were not stated. Hourman [19] analyzed performance of DP steels for side intrusion rail, which deforms primarily in bending.

The U. S. Auto/Steel Partnership has been developing automotive steels for a wide range of dynamic conditions. Strain-rates from quasi-static values (0.001/s) to high velocity dynamic impact using split Hopkinson bar experiments (1000+ /s) were considered [13]. Mahadevan et al. [13] used the developed dynamic material data and employed it for FEM simulation of crush experiments of various tubular steel geometries using Johnson-Cook [20] and Zerilli-Armstrong [21] material models. They concluded that higher fidelity correlation was achieved with the Johnson-Cook model and that the modeling, especially, finite element discretization, had a significant effect on the results. In the follow-up paper [22], Mahadevan et al. investigated effects of strain-rate in full vehicle frontal crash analysis and have analyzed the effects of various material model fitting strategies and element discretizations. The material information from A/SP research was made available to this project and was used for the development of advanced HSS material models for ULSAB. The first task involved pairing of the ULSAB materials and available materials from the A/SP project. Figure 9 shows the quasi-static properties of the materials used in the A/SP study.

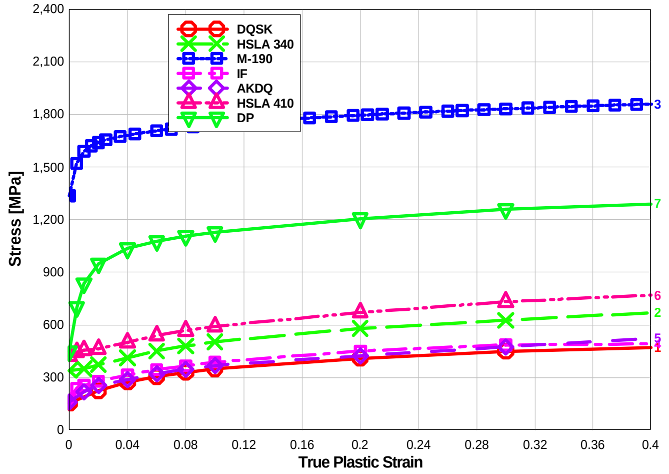

Figure 9. Quasi-static Material Properties from A/SP.

The quasi-static material properties from A/SP were related to ULSAB material properties used in the crash model (Figure 8). Table 1 shows how the materials were substituted. Modification of material properties to match exactly the yield points [2] was considered, however they were not used because the overall fit between the respective strain-stress curves was adequate.

ULSAB Mat. ID	Yield Stress [MPa]	A/SP Mat. Substitute	A/SP Yield Stress [MPa]
1	350	HSLA	340
2	210	DQSK	155
3	195	DQSK	160
4	600	DP	450
5	420	HSLA	425
6	276	IF	180
7	872	M-190	1336

Table 1. Pairing of ULSAB and A/SP Tested Materials.

As can be seen from the table, some of the materials have yield values significantly higher than is customarily expected for those steel designations. The yield values may have been increased in the original quasi-static model in order to include experience that the designers had with the modeling of the dynamic behavior of these materials and automotive structures. Properties of the substituted materials under different strain-rates were used as input data for the piece-wise-linear plasticity model in LS-DYNA3D (material 24 with strain-rate table option). In this model, true strain-true stress curves for different strain-rates are tabulated, and computed equivalent plastic strains and strain-rates are then interpolated between the values in the table to determine the equivalent plastic stress. Material data for material designated as HSLA 1 is shown in Figure 10.

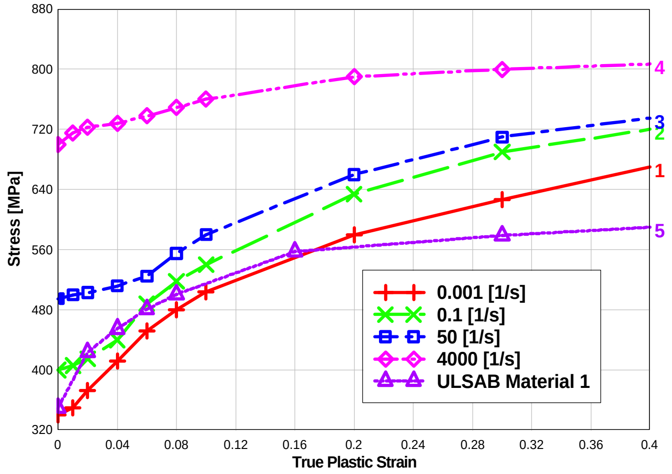

Figure 10. Strain-rate Material Properties for HSLA 1.

It is evident from the character of the curves in Figure 10 that they do not have the same hardening rates across the strain-rates and as such would be difficult to fit to the constitutive models that are based on that assumption. Obvious questions on the effects of differences in the experimental hardening rates and accuracy of the measured responses in the context of crashworthiness models still need to be answered. These and other modeling and experimentation issues, are presently addressed by the research within the A/SP and the U.S. Department of Energy.

CRASHWORTHINESS SIMULATIONS

The ULSAB model with new material properties was used for various crash simulations to investigate effects of advanced material modeling on computational results. Only the results from the NCAP crash simulations are presented in this paper because they suffice for illustration of the main trends that are observed across different impact scenarios. During the course of the project, a large number of impact scenarios and material modeling approaches has been considered. These simulations result in large amounts of data that tend to overwhelm the analyst. A new interactive, Web-based problem solving environment system has been developed to facilitate analysis between remote project participants [23]. A set of characteristic locations has been selected for monitoring displacements and accelerations. Cross-section forces and displacements on several positions have also been used to assess the magnitude and dynamic of forces in main crash structures. The locations of the data points, cross-sections and components are shown in Figure 11.

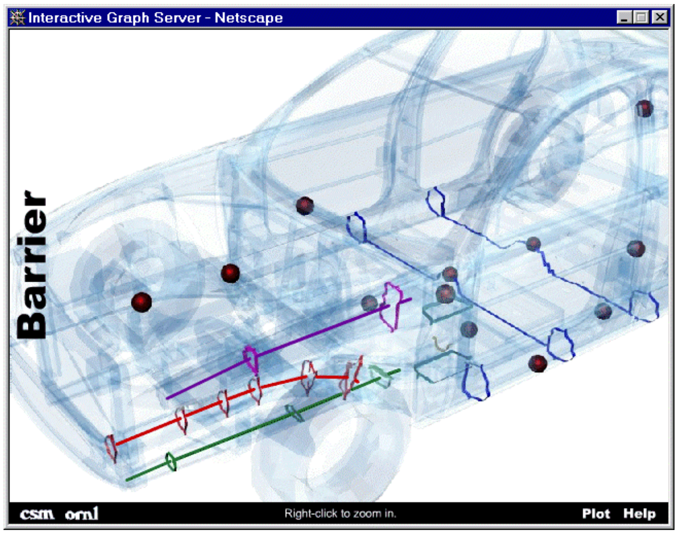

Figure 11. Data Acquisition Locations.

Red (dark) spheres are associated with displacement and acceleration data, cross sections are associated with forces in the direction perpendicular to the cross section and lines are associated with collapse measures of the structural components.

NCAP crash simulations for vehicle models with and without material strain-rate sensitivity were performed. Filtered (SAE J211) acceleration traces for the node at the rocker near the bottom of B-pillar are shown in Figure 12.

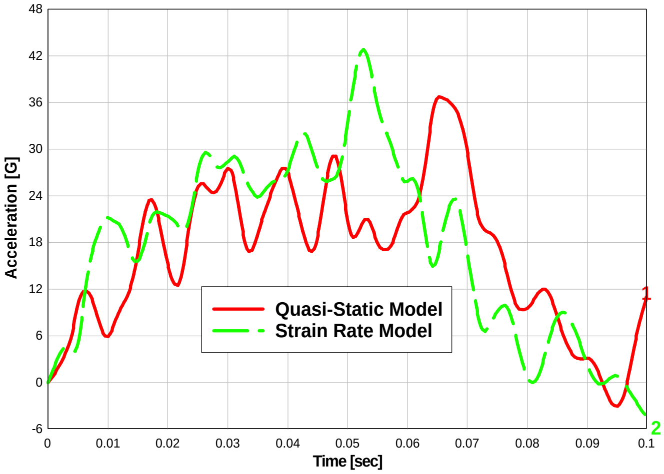

Figure 12. Acceleration at Rocker near B-pillar.

This point on the vehicle is usually used as a link between occupant environment and the vehicle dynamics models. Crash pulses on the rocker are transferred from one model to another to determine crashworthiness of a design. On average, the acceleration levels for material modeling with strain-rate sensitivity are compared to the simulations using quasi-static material models. The average acceleration for two cases between the impact start, $\boldsymbol{t}_0$ (“time zero”), and the end of the forward movement of the vehicle $\boldsymbol{t}_{v=0}$ (“velocity zero”), are 19.9 G and 23.5 G, respectively. The trend is consistent across the vehicle points. The longitudinal displacement of the point on the floor of the vehicle is shown in Figure 13.

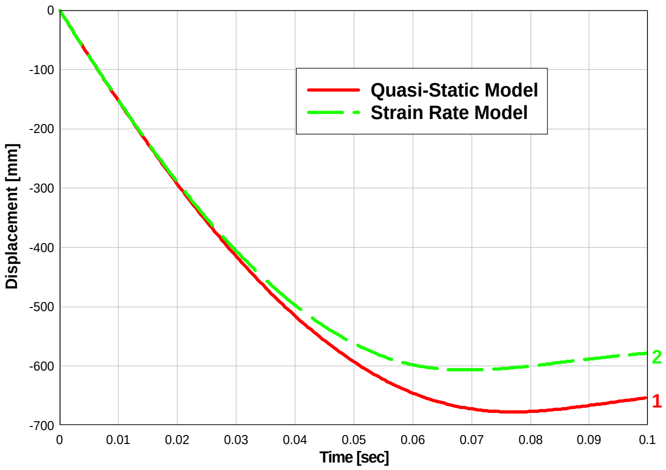

Figure 13. Displacement of Car Center.

The strain-rate sensitivity results in 11% reduced displacement and shorter vehicle stopping time. The results are consistent with values reported in the literature [22]. The higher accelerations and shorter stopping distance come from the increase in rail forces due to the strain-rate sensitivity of the material. The force in the rear of the lower rail is shown in Figure 14.

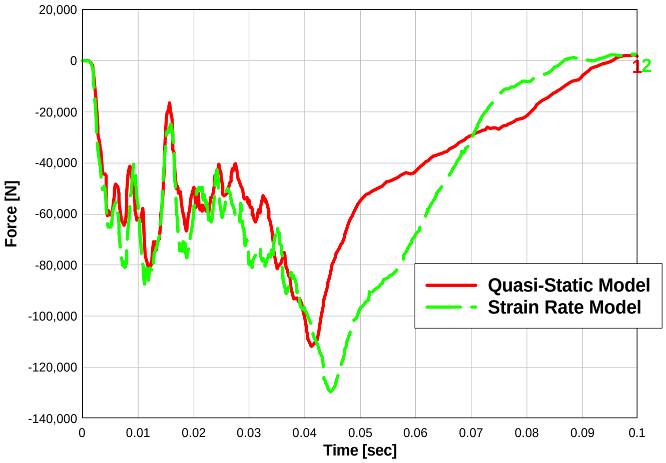

Figure 14. Force in Lower Rail.

Not only does the strain-rate sensitivity increase the force peak in the lower rail, it also extends its duration, which results in more energy dissipation of the component. The average force between the “time zero” and “velocity zero” in the rail for quasi-static case is 52.6 kN and for the strain-rate model is 70.1 kN (33% increase). Figures 15 and 16 show deformation of the lower rail at 80 ms.

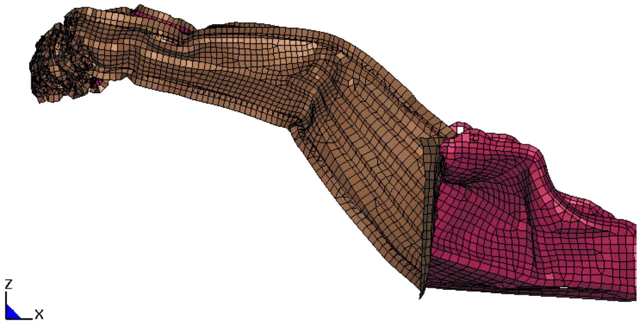

Figure 15. Lower Rail - Quasi-static Model.

Figure 16. Lower Rail – Strain-rate Model.

The quasi-static model has a pronounced plastic hinge near the middle of the rail. This hinge is created just after .04 seconds, which corresponds to the significant loss of load carrying capacity of the lower rail in the quasi-static model as seen in Figure 14.

The use of the strain rate material model influences the energy management prediction relative to the static material model in two ways. An incremental advantage is predicted due to the increased flow stress of the strain rate model when the structure is predicted to collapse in a similar manner to that predicted by the quasi-static model. This is seen in Figure 14 prior to .04 seconds and corresponds to the similar folding of the leading edge of the rail for both material models. However, after .04 seconds the two material models predict a significantly difference collapse modes of the lower rail. A pronounced hinge is predicted to form near the middle of the rail for the quasi-static model. The creation of this hinge at .04 seconds predicts a significant reduction in the energy management capacity of the lower rail as shown in Figure 14

The structural response of the lower rail has to be viewed in the context of the entire design. Figure 17 shows the response of upper and lower rails for different material models.

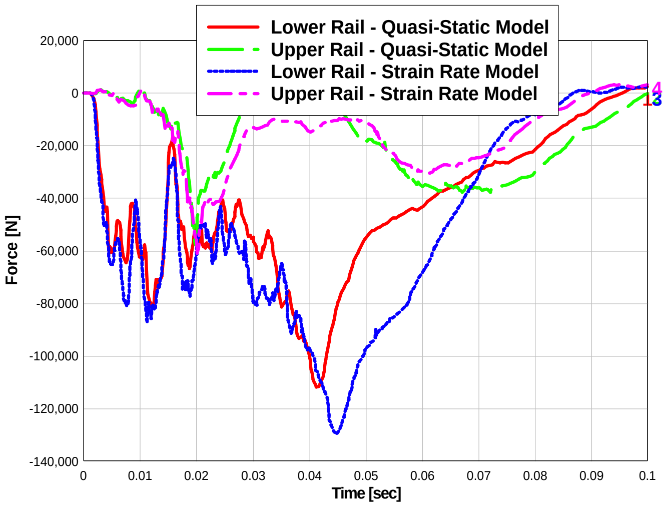

Figure 17. Forces in Upper and Lower Rails

Average force in the upper rail remains almost the same (changes less than 1%). Addition of more force traces in the graph would quickly make the graph too crowded for illustration of global trends. Corresponding deformation of the front crash system as shown in Figures 18 and 19, provides a good illustration of the overall trend.

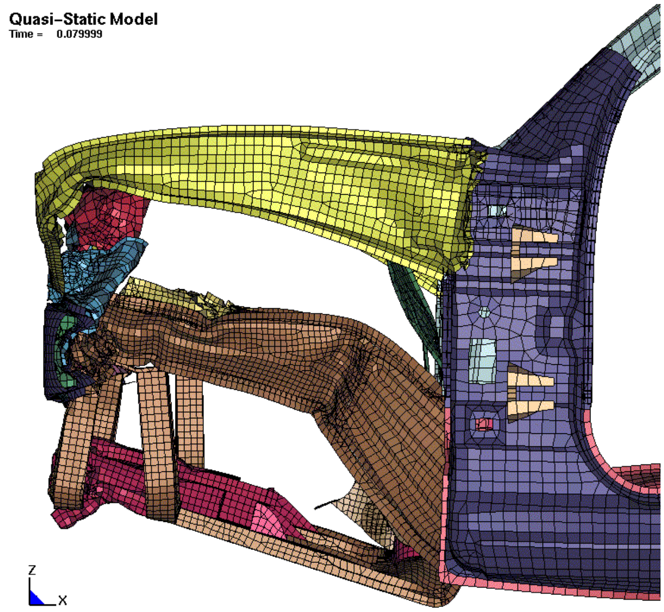

Figure 18. Deformation of Rails for Quasi-Static Model.

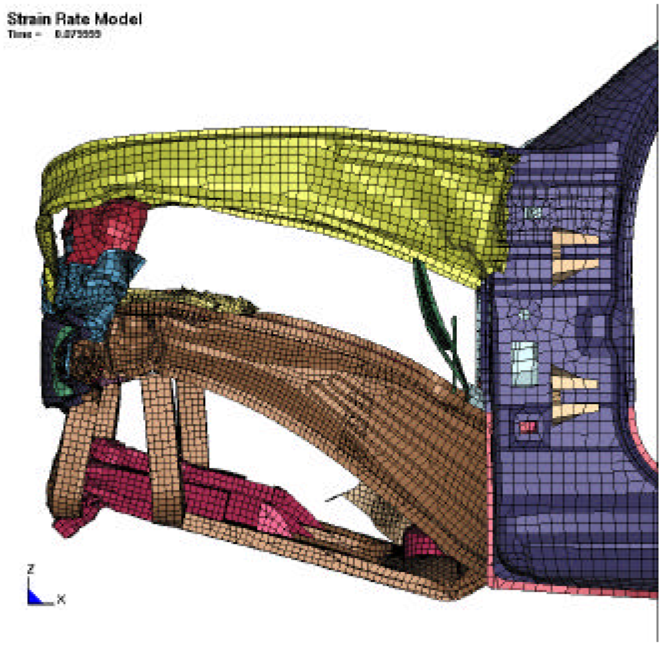

Figure 19. Deformation of Rails for Strain-rate Model.

Overall a shorter crush zone, and less localization into plastic hinges are the two most prominent effects of strain-rate in the above figures. Other views reveal that the amount of forward pitching of the occupant compartment, as indicated by the angle of the hinge-pillar, is larger for the quasi-static case.

As the advance in computer hardware allows for ever more detailed and finer element discretizations, data interpretation on the component level quickly becomes a problem. To consolidate the simulation results into measurable representation, two collapse deformation measures for the components (upper and lower rails and sub-frame) were defined. The first measure is defined as the distance between the centroids of the end cross sections of the component. The second measure is defined as the sum of distances between the consecutive cross sections on the component. For a sufficient number of cross sections, the compactness of the collapse process will be indicated by the small difference between the two measures. These measures integrate information about large material volumes and can be shown in a single graph. In addition, they can provide a link between semi-empirical design tools and FEM approaches. More detailed collapse measures are currently being developed and will be included in the later publications on the subject. The two collapse measures of the lower rail are shown in Figure 20.

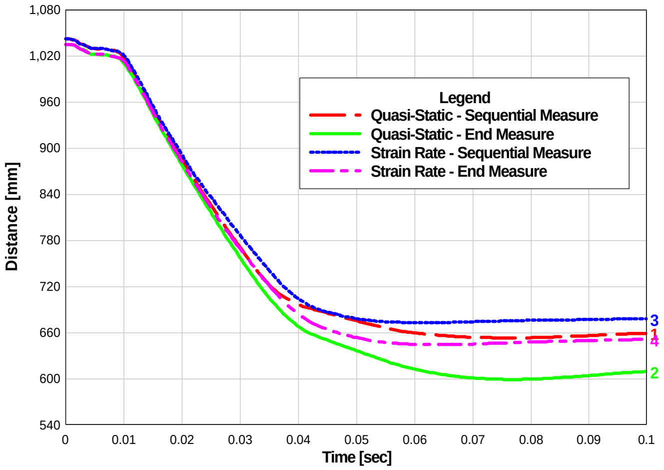

Figure 20. Lower Rail Collapse Measures.

Similar to the displacement data in Figure 13, the strain-rate sensitivity results in the overall shorter collapse. The difference between the end and sequential collapse measures is smaller for the strain-rate sensitive model which indicates a more compact collapse. Similarly to the force analysis, it is necessary to consider the entire rail system that is shown in Figure 21.

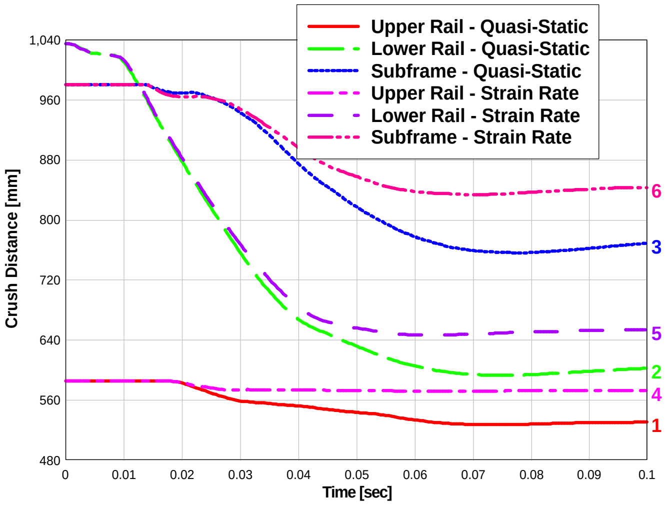

Figure 21. Collapse of Rails and Subframe.

Overall, the crush of the entire rail system is shorter and the strain-rate effect is significant enough that it should be considered in the detailed vehicle impact analysis. (Note that the upper rail involves cross sections as shown in Figure 11, and does not include deformation in the front end.) The reader is reminded at this point that the previous conclusions are based mostly on computational simulations and have not been verified by the physical crash experiment. Nevertheless, the objective of the study remains valid. Simulation results clearly indicate that the strain-rate is an important factor that can have considerable effect on overall vehicle response and, thus, provides further rationale support for experimental and theoretical investigation of the subject.

MATERIAL SUBSTITUTION ANALYSIS

ULSAB material selection depended to a large extent on material yield characteristics, as it is customary in the current car design. Elasto-plastic response characteristics of conventional mild steel materials have been generally conformant to this assumption. To investigate the effect of material substitution of the HSS intensive design, using materials of similar yield but different strain-rate and hardening characteristic HSLA 340 of Figure 1 is substituted with DP 430. The strain-rate dependent material data for lower DP grades was not available so the closest material available was used [24]. In addition, the yield point for DP steels is not easily determined since it just presents a point on the very steep hardening curve. Material data for the two materials is shown in Figure 22.

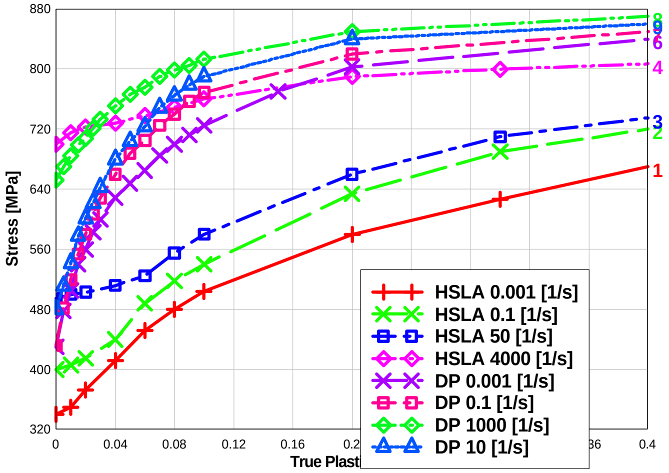

Figure 22. Comparison of Substituted Material Properties.

CRASHWORTHINESS SIMULATIONS

Displacement and accelerations in the car center, and rail collapse measures are shown in Figures 23 to 25, respectively.

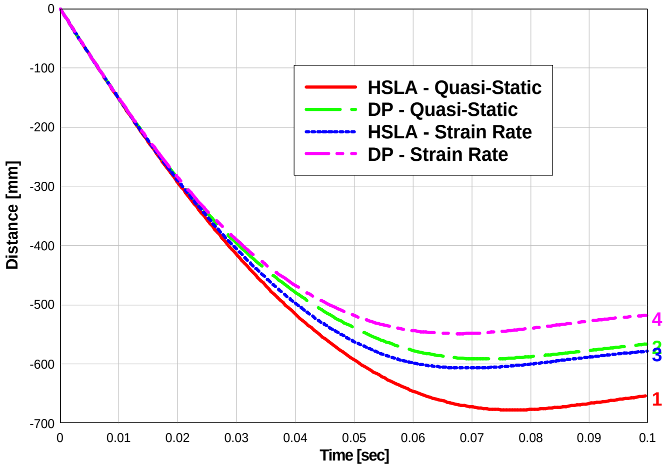

Figure 23. Displacements of Car Center.

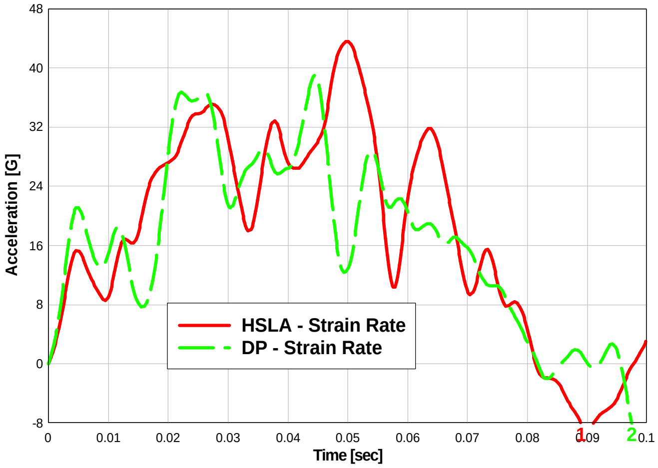

Figure 24. Accelerations of Car Center.

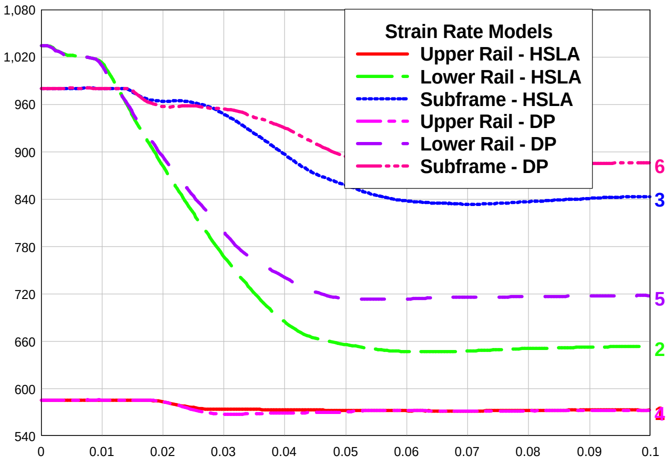

Figure 25. Rail Collapse.

It is interesting to observe that even though the accelerations are very similar, the displacements and collapse measures are not. DP material is intrinsically less strain-rate sensitive when compared to HSLA and, therefore, differences between material models are less pronounced (see Figure 23). The load paths have been appreciably influenced in the lower rail and sub frame, while upper rail deformation is very similar to the original design.

CONCLUSIONS

Crash modeling simulations show a clear effect of strain-rate sensitivity on high strength steel (HSS) intensive vehicle. The influence of a strain-rate model can be an incremental sensitivity due to the increased flow stress when similar structure collapse modes are predicted. However, significant differences in crash energy management capacity can be predicted if the change in loading on members alters the predicted collapse mode of the structure. From the material substitution study it can be concluded that HSS material substitution cannot be performed on the basis of the material yield point only and that, especially for advanced HSS vehicle designs, the entire region of material plastic response has to be considered. However, the problem of modeling of the overall dynamic crush process still remains open and requires further experimental and theoretical investigation.

ACKNOWLEDGMENTS

The research discussed in this paper is sponsored by the American Iron and Steel Institute (AISI) under Project Number ERD-97-XM001 with the U.S. Department of Energy. Work was performed at the Oak Ridge National Laboratory (ORNL), which is managed by UT-Battelle, LLC for the U.S. Department of Energy under contract DE-AC05-00OR22725.

The authors wish to thank the Safety Panel of AISI for their support in writing this paper. In addition to that the authors would like to thank Jon Harrington from AISI for reviewing the paper. They also would like to thank the Automotive Applications Committee of AISI as well as management of ORNL for granting the opportunity to submit this paper. Lastly, the ULSAB consortium needs to be recognized for granting permission to use the ULSAB study - the project was conducted by Porsche Engineering Services, Inc. and finished in 1998 - as basis for the work done by ORNL.

The American Iron and Steel Institute (AISI) is a non-profit association of North American companies engaged in the iron and steel industry. The Institute comprises 47 member companies, including integrated and electric furnace steelmakers, and 178 associate and affiliate members who are suppliers to or customers of the steel industry. Member companies account for more than two-thirds of the raw steel produced in the U.S., most of the steel manufactured in Canada and nearly two-thirds of the flat-rolled steel products manufactured in Mexico. For a broader look at steel and its applications, the Institute has its own web site at http://www.steel.org.

CONTACT

For additional information on details on the research project please contact Srdan Simunovic, simunovics@ornl.gov. Dr. Simunovic is a materials research engineer in the Computational Materials Science Group (http://www-cms.ornl.gov) at the Oak Ridge National Laboratory. For additional information on the scope and other AISI related areas please contact Marcel van Schaik, vanschaikm@autosteel.org. Marcel van Schaik is Manager, Advanced Materials Technology at the American Iron and Steel Institute.

REFERENCES

1 Ultralight Steel Auto Body Final Report, Porsche Engineering Services, Inc. March, 1998.
2 Paluszny, A., State-of-the-art review of automobile structural crashworthiness, AISI publication AU2301 (1051), 1993.
3 Jones, N., Structural Impact, Cambridge University Press 1989.
4 Constitution and Properties of Steels, vol. ed. Pickering, F. B., Materials Science and Technology, vol. 7, VCH, New York, 1992.
5 Crisfield, M. A., Advanced Topics, Volume 2, Non-Linear Finite Element Analysis of Solids and Structures Non-Linear Finite Element Analysis of Solids and Structure, Wiley, 1997.
6 Belytschko, T., Liu, W. K., Moran, B., Nonlinear Finite Elements for Continua and Structures, Wiley, 2000.
7 Campbell, J. D., Dynamic Plasticity of Metals, Springer, New York 1972.
8 Davies, R. G. and Magee, C. L., The Effect of Strain-Rate Upon the Tensile Deformation of Materials, Journal of Engineering Materials and Technology, April 1975, pp. 151-155.
9 Davies, R. G. and Magee, C. L., The Effect of Strain-Rate Upon the Bending Behavior of Materials, Journal of Engineering Materials and Technology, January 1977, pp. 47-51.
10 Kassar, M.; and Yu, W.W., Effect of strain-rate on material properties of sheet steels, Journal of Structural Engineering v 118 n 11 Nov 1992 pp. 3136-3150.
11 Kassar, M.; Pan, C.L.; Yu, W.W., Effect of strain-rate on cold-formed steel stub columns, Journal of Structural Engineering Vol. 118 n 11 Nov 1992 pp. 3151-3168.
12 Thornton, P. H., Energy Absorption by Structural Collapse in Dual Phase Steel Tubes, Metallurgical Transactions A, Vol. 10A, 1979.
13 Mahadevan, K., Fekete, J. R., Schell B., McCoy, R., Faruque, O., Strain-Rate Characterization of Automotive Steel and the Effect of Strain-Rate in Component Crush Analysis, SAE paper 982392, 1998.
14 Hallquist, J. O., LS-DYNA3D, An explicit finite element nonlinear analysis code for structures in three dimensions, LSTC Manual, 1995.
15 Geoffroy, J.L.; Cambien, I.; Jouet, A., Contribution of high strength steels to the absorption of impact energy, Metallurgia Italiana v 85 n 6 Jun 1993 p 377-382.
16 Yoshitake, Sato, K., A. Hosoya, Y., A study on improving crashworthiness of automotive parts by using high-strength steel sheets, SAE paper 980382, 1998.
17 Sato, K., Yoshitake, A. Hosoya, Y., Mikami, H., FEM Simulation to Estimate Crashworthiness of Automotive Parts, SAE paper 982356, 1998.
18 Miura, K., Takagi, S., Hira, T., Furukimi, O. Tanimura, S., High strain-rate deformation of high-strength sheet steels for automotive parts, SAE paper 980952, 1998.
19 Hourman, T., Press forming of high strength steels and their use for safety parts, Revue de Metallurgie. Cahiers D'Informations Techniques v 96 n 1 1999. p 121-132 0035-1563
20 Johnson, G. R. and Cook, W. H., A Constitutive Model and Data for Metals Subjected to Large Strains, High Strain-rates and High Temperatures, *Proceedings of the Seventh International Symposium on Ballistic*, The Hague, The Netherlands, 1983, pp. 541-547.
21 Zerilli, F. J. and Armstrong, R. W., Dislocation-Mechanics-Based Constitutive Relations for Material Dynamics Calculations," Journal of Applied Physics V 61 (5), pp. 1816-1825, 1987.
22 Mahadevan, K., Fekete, J. R., Liang, P., Effect of Strain-rate in Full Vehicle Frontal Crash Analysis, SAE paper 2000-01-0625, 2000.
23 Bobrek, A., Simunovic, S., Aramayo, G., Collaborative Toolkit for Crashworthiness Research HICSS-34, Minitrack on Developing and Deploying Collaborative Problem Solving Environments 2001.
24 Yoshitake, A.; Sato, K.; Okita, T., Impact absorbed energy of hat square column in high strength steels, SAE International Congress & Exposition Feb 26-29 1996 n1172 1996 Detroit, MI, USA, SAE Warrendale PA USA p 7 0099-5908 SAESA2.